Supporting Information

An Intrinsically Stretchable and Ultrasensitive Nanofiber-Based Resistive Pressure Sensor for Wearable Electronics

Fang-Cheng Liang[a,b,+], Hau-Jen Ku[a,+], Chia-Jung Cho[a], Wei-Cheng Chen,[a] Wen-Ya Lee[c], Wen-Chang Chen[d], Syang-Peng Rwei[a], Redouane Borsali[b,*], and Chi-Ching Kuo[a,*]

[a] Institute of Organic and Polymeric Materials, Research and Development Center of Smart Textile Technology, National Taipei University of Technology, No. 1, Sec. 3, Chung-Hsiao East Road., Taipei, 10608, Taiwan (R.O.C.)

[b] Centre de Recherches sur les Macromolécules Végétales (CERMAV), affiliated with Grenoble Alpes University, Institut Carnot PolyNat, BP53, 38041 Grenoble Cedex 9, France

[c] Department of Chemical Engineering and Biotechnology, National Taipei University of Technology, 10608 Taipei, Taiwan (R.O.C.)

[d] Department of Chemical Engineering, Advanced Research Center for Green Materials Science and Technology, National Taiwan University, 106 Taipei, Taiwan (R.O.C.)

+F.-C. Liang and H.-J. Ku contributed equally to this work.

*Author to whom all correspondence should be addressed

Tel.: 886-2-27712171*2407; Fax: 886-2-27317174

Correspondence to: Prof. C.-C. Kuo (E-mail: kuocc@mail.ntut.edu.tw)

Dr. R. Borsali (E-mail: borsali@cermav.cnrs.fr)

Experimental section

Materials

A linear triblock copolymer SEBS (G1652) (Mn = 79000 g/mol^{-1}, weight fraction of styrene = 30%) was purchased from Kraton, and $AgCF_3COO$ (98%), hydrazine hydrate ($N_2H_4 \cdot 4H_2O$, ~50−60%), N, N-dimethylformamide (DMF, 99.5%), ethanol (95.0%), and tetrahydrofuran anhydrous (THF, 99.9%) were purchased from Sigma Aldrich. Tetra-n-butylammonium perchlorate (99%) was purchased from Alfa Aesar.

Preparation of SEBS fiber and AgNPs composites

SEBS was dissolved in a tetrahydrofuran anhydrous and dimethylformamide (THF/DMF) solvent to adjust the concentration of 12 wt% and stirred overnight. Tetra-n-butylammonium perchlorate (4 wt% of the solute) was added to the polymer solution, which was electrospun onto the collector with a feed rate (1 mL/h) and voltage (14.0 kV) during electrospinning. A piece of aluminum foil or quartz was placed 15 cm below the tip of the needle to collect the nanofibers. The SEBS fiber mat was carefully peeled away from the collector and then directly dipped in a silver precursor solution (5 wt% $AgCF_3COO$ in ethanol). The fiber mats were subtly removed from the silver precursor solution after 30 mins and dried at room temperature. A mixture of 50% Hydrazine hydrate was prepared by water: ethanol (1:1 volume ratio) solvent and then directly dropped onto the fiber mat until the solution was fully absorbed by fiber mat. The residual agents were washed out with deionized water several times after 10 mins.

Design and fabrication of the skin-inspired ESSCN pressure sensor

The same proportion of the SEBS polymer solution was electrospun onto the collector gap (length of 3 cm and gap width of 1 cm) to form a SEBS dielectric layer. The feed rate was fixed at 1 mL/h and the spinning voltage was set at 14 kV. The nozzle-to-collector distance was 15

cm. The SEBS dielectric layer was controlled with different electrospinning times (1, 2, and 3 min), and designated as SEBS-1, SEBS-2, and SEBS-3, which were transferred to the SEBS/AgNP fiber mat. As shown in **Fig. 1** and **Fig. S10**, two assembled of SEBS/AgNP composites were formed by face-to-face into a resistive pressure sensor and each of the thin films was glued with silver paste onto the two copper wires as electrodes, yielding the interplane current paths.

Characterization of skin-inspired ESSCN pressure sensor

The ultraviolet-visible spectrophotometer was used for recording Ultraviolet spectra. FT-IR spectra were recorded using a Bio-Rad 155 FT-IR spectrometer at ambient temperature in the range of 650−4000 cm^{-1}. The XRD patterns recorded on an X-ray diffractometer (D8 ADVANCE, Bruker, Germany) were used for elemental analysis of SEBS/AgNP fibrous electrodes. A stress−strain curve was obtained using a universal tensile stress testing machine (Taiwan Research and Development Center Institute). The morphology and elemental components of the samples were investigated by FE-SEM (Hitachi S-520) equipped with EDX spectroscopy. The resistance curves, response times, detection ranges, and mechanical stimuli of the pressure sensors were measured with a Keithley 2634B analyzer by using the silver paste to glue with two copper onto the thin-film electrodes. The cyclic loading-unloading measurement was performed with the computer-controlled movable stage (ShanduSJS-500V) and force gauge (Shandu SH-500B). As shown in **Fig. S5**, the custom-built device was designed to investigate the responses of the sensors to static pressures, enabling them to perform with repeatedly applied and released capability on the pressure sensors at a certain constant pressure based on a linear motor system. The biomedical monitoring is using a commercially available transparent elastomer tape (VHB 4905, 3M). The real-time demonstration of the circuit was completed by integration with RGB-LED garments and health-monitoring devices (**Movie S1 and Movie S2**).

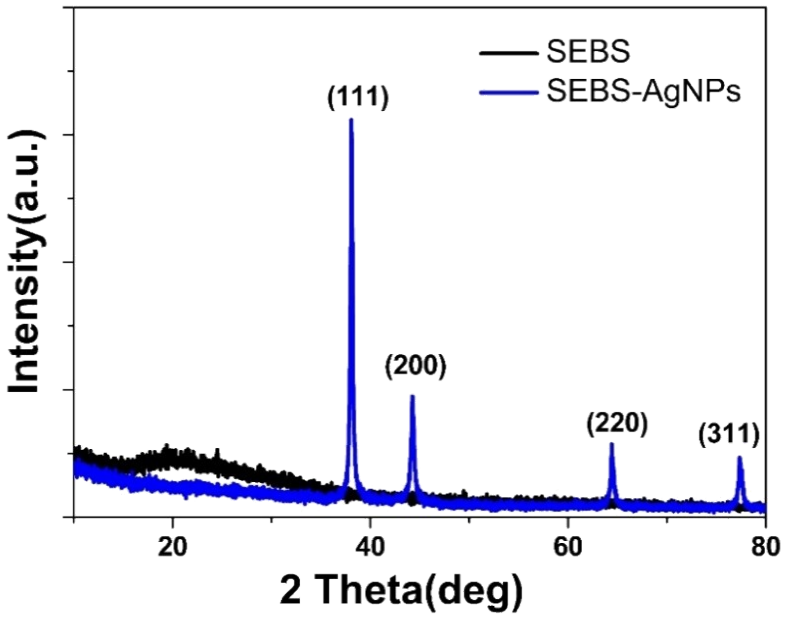

Fig S1. XRD patterns of SEBS and SEBS-AgNPs

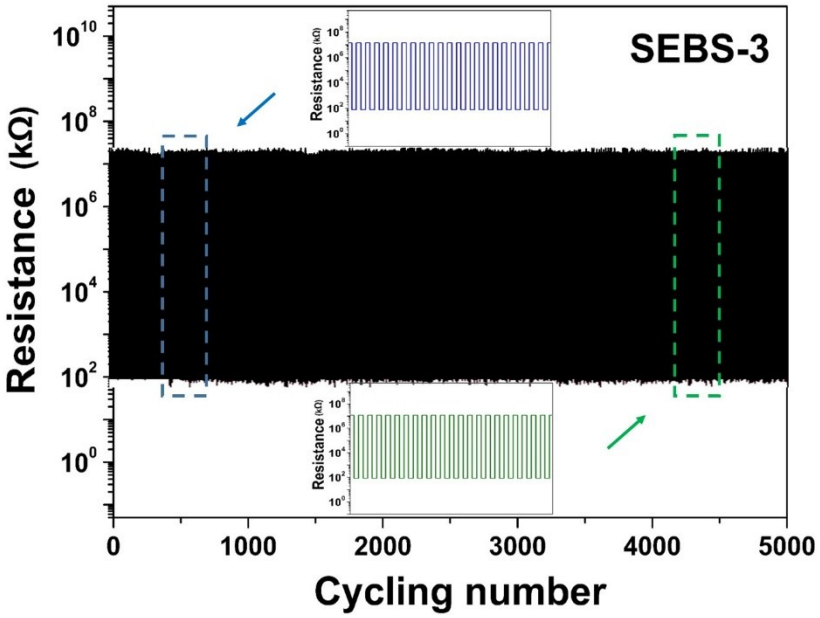

Fig S2. Stability test of the SEBS-3 pressure sensor under pressure of 22.02 kPa over 5000 loading-unloading cycles.

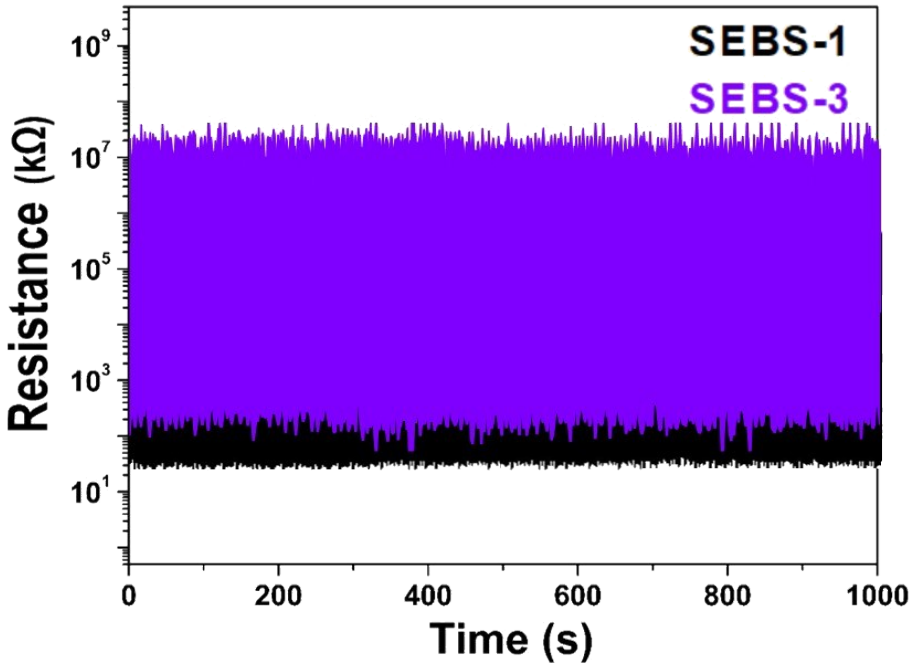

Fig S3. Repeatability response resistance values of SEBS-1 and SEBS-3 pressure sensors under pressure of 0.18 kPa and 22.02 kPa under loading-unloading cycle tests.

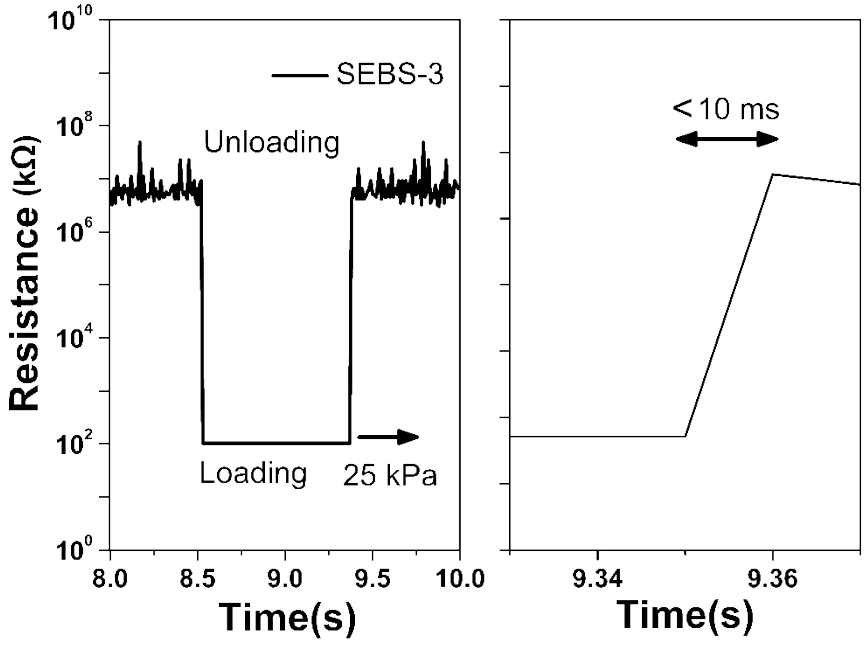

Fig S4. Response time of the SEBS-3 pressure sensor with an applied pressure of 25 kPa and instant response time of within 10 ms (the right figure shows the magnified curve of the left one).

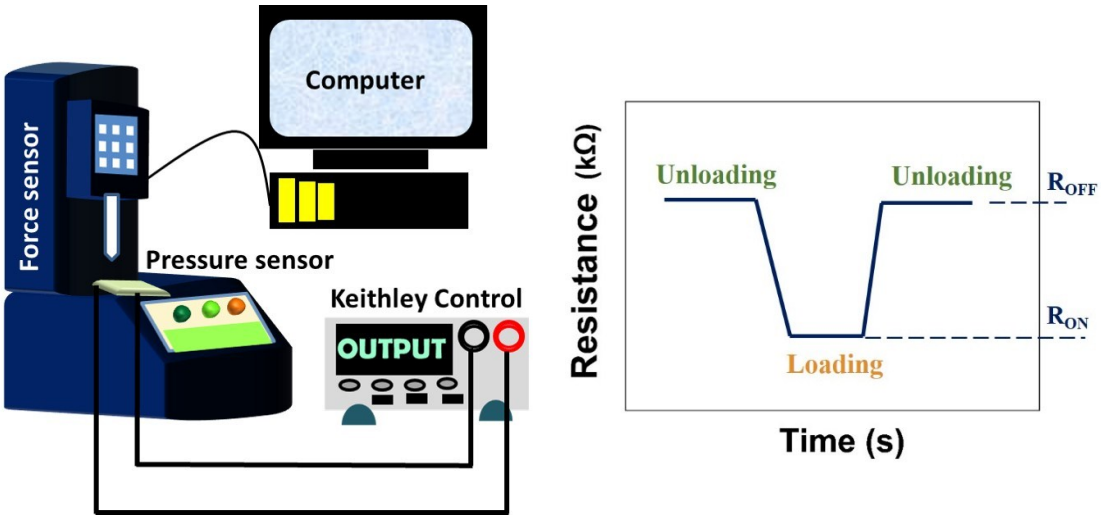

Fig S5. Schematic of the system of the pressure sensing measurement and the illustration of resistance change in responses of loading and unloading test with ESSCN pressure sensors.

The total resistance calculations are associated with the resistance of AgNPs electrode (R_S) and the resistance of dielectric SEBS nanofibers (R_P). The corresponding resistance change can be defined as $(R_0 - R) / R_0 = (R_{S0} - R_S + R_{P0} - R_P) / (R_{S0} + R_{P0})$, R_{S0} and R_{P0} represent initial resistance value of AgNPs electrode and dielectric SEBS nanofibers, respectively. Notably, the R_{S0} with high conductive performance is much smaller than R_{P0}, result in the minimum resistance variation ratios of AgNPs electrode ($R_{S0} - R_S$). Hence, the total resistance change ($(R_0 - R) / R_0$) can be equally as $(R_{P0} - R_P) / R_{P0}$, indicating that the sensitivity of ESSCN pressure sensors relies on resistance variation ratios of dielectric SEBS nanofibers between the two AgNPs electrode".

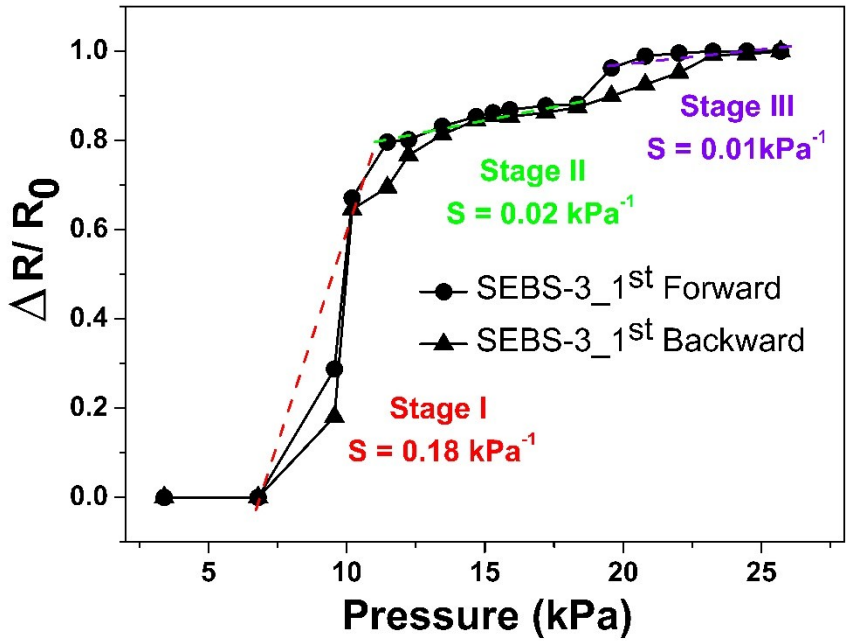

Fig S6. Plots of relative resistance change ($\Delta R/R_0$) of the SEBS-3 pressure sensor as a function of loading force under pressure.

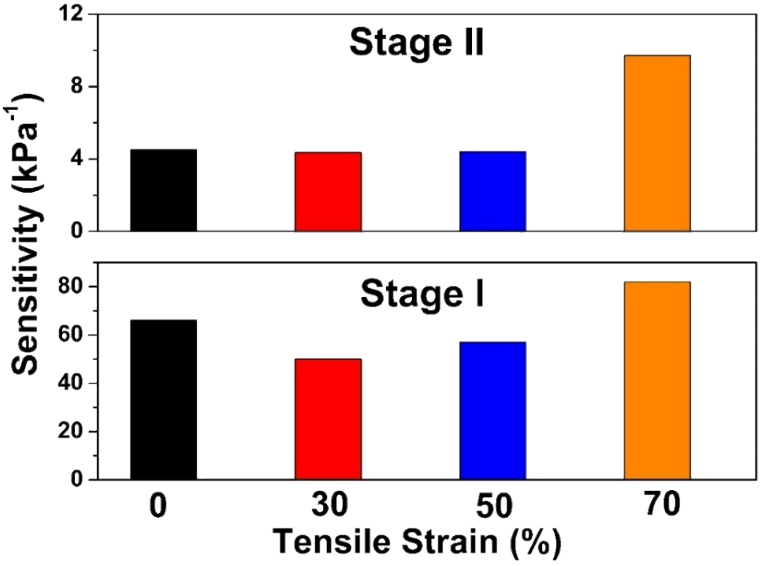

Fig S7. Sensitivities of the sensor under various tensile strains in stages I and II, obtained from the slopes of the curves in Fig 3g.

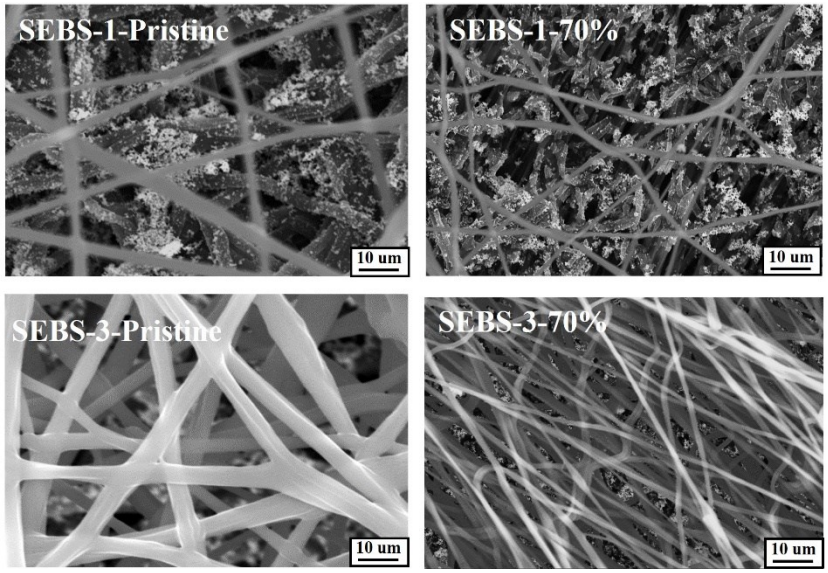

Fig S8. SEM images of SEBS-1 and SEBS-3 composites before stretching and after applying 70% tensile strain.

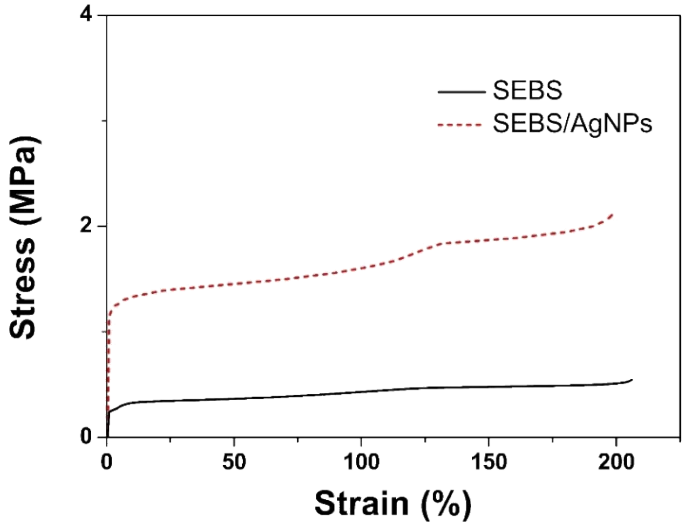

Fig S9. Stress−strain curves of SEBS and SEBS-AgNP composites.

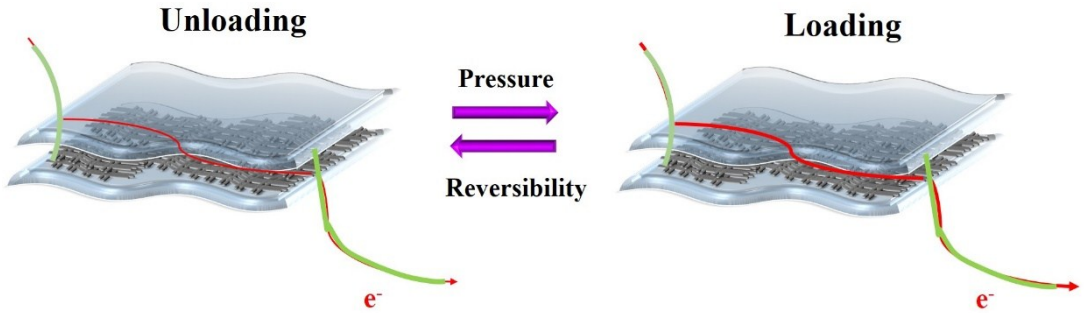

Fig S10. Schematic illustrations of the ESSCN pressure sensors.

Table S1. Comparison of this study and previous flexible pressure sensors.

Type of Devices	Materials	Sensitivity	Response time	References
Piezoelectric	PZT	2 $\mu A \cdot Pa^{-1}$	0.1	1
Piezoelectric	ZnO nanorod	2.1 $\mu S \cdot kPa^{-1}$	150	2
Piezoelectric	PVDF	0.2 $V \cdot kPa^{-1}$	-	3
Piezoelectric	P(VDF-TrFE) Nanofiber	0.41 $V \cdot Pa^{-1}$	-	4
Capacitance	Graphene oxide	0.8 kPa^{-1}	~100	5
Capacitance	AgNWs/PDMS	2.94 kPa^{-1}	<50	6
Capacitance	Porous PDMS	1.5 kPa^{-1}	-	7
Capacitance	AgNWs/PVDFNM	4.2 kPa^{-1}	<26	8
Capacitance	AgNW/ moulded PDMS	3.8 kPa^{-1}	<150	9
Capacitance	Ag/PDMS	1.45 MPa^{-1}	100	10
Piezoresistive	Graphene/polyimide	0.045 kPa^{-1}	<700	11
Piezoresistive	CNT /Paper	2.2 kPa^{-1}	35~40	12
Piezoresistive	Lotus leaf/PDMS	1.2 kPa^{-1}	-	13
Piezoresistive	MoS_2	0.011 kPa^{-1}	180	14
Piezoresistive	AgNWs/PU	4.1 kPa^{-1}	55	15
Piezoresistive	CNT/ PDMS	0.101 kPa^{-1}	<10	16
Piezoresistive	CNT/ PDMS	10.8 kPa^{-1}	<10	17
Piezoresistive	Foam/ PDMS	0.67 kPa^{-1}	<10	18
Piezoresistive	CNT/ Textile	0.31 kPa^{-1}	<20	19
Piezoresistive	CNT / PDMS	0.21 kPa^{-1}	<1200	20
Piezoresistive	SWNTs/PDMS	1.8 kPa^{-1}	<10	21
Piezoresistive	Au NWs/tissue paper	1.14 kPa^{-1}	<17	22
Piezoresistive	**SEBS/AgNPs**	**71.07 kPa^{-1}**	**<2**	**This work**

Notes and references

1. C. Dagdeviren, Y. Su, P. Joe, R. Yona, Y. Liu, Y.-S. Kim, Y. Huang, A. Damadoran, *Nat. Commun*., 2014, **5**, 4496.
2. W. Wu, X. Wen, Z. L. Wang, *Science,* 2013, **340**, 952.
3. A. B. Joshi, A. E. Kalange, D. Bodas, S. Gangal, *Mater. Sci. Eng. B* **2010**, *168*, 250-253.
4. L. Persano, C. Dagdeviren, Y. Su, Y. Zhang, S. Girardo, D. Pisignano, Y. Huang, J. A. Rogers, *Nat. Commun,*. 2013, **4**, 1633.
5. S. Wan, H. Bi, Y. Zhou, X. Xie, S. Su, K. Yin, L. Sun, *Carbon,* 2017, **114**, 209.
6. X. Shuai, P. Zhu, W. Zeng, Y. Hu, X. Liang, Y. Zhang, R. Sun, C. Wong, *ACS Appl. Mater. Interfaces,* 2017, **9**, 26314.
7. S. Park, H. Kim, M. Vosgueritchian, S. Cheon, H. Kim, J. J. Koo, T. R. Kim, S. Lee, G. Schwartz, H. Chang, *Adv. Mater.,* 2014, **26**, 7324.
8. W. Yang, N.-W. Li, S. Zhao, Z. Yuan, J. Wang, X. Du, B. Wang, R. Cao, X. Li, W. Xu, Z. L. Wang, C. Li, *Adv. Mater. Technol.,* 2017, **3**, 1700241.
9. Y. Joo, J. Byun, N. Seong, J. Ha, H. Kim, S; Kim, T. Kim, H. Im, D. Kim, Y. Hong, *Nanoscale,* 2015, **7**, 6208.
10. X. Zhao, Q. Hua, R. Yu, Y. Zhang, C. Pan, *Adv. Electron. Mater.,* 2015, **1**, 1500142.
11. M. A. S. M. Haniff, S. M. Hafiz, N. M. Huang, S. A. Rahman, K. A. A. Wahid, M. I. Syono, I. A. Azid, *ACS Appl. Mater. Interfaces,* 2017, **9**, 15192.
12. Z. Zhan, R. Lin, V. Tran, J. An, Y. Wei, H. Du, T. Tran, W. Lu, *ACS Appl. Mater. Interfaces,* 2017, **9**, 37921.
13. J. Shi, L. Wang, Z. Dai, L. Zhao, M. Du, H. Li, Y. Fang, *Small,* 2018, **14**, 1800819.
14. Y. J. Park, B. K. Sharma, S. M. Shinde, M. S. Kim, B. Jang, J. H. Kim, J. H. Ahn, *ACS Nano,* 2019, **13**, 3023.
15. X. Liao, W. Song, X. Zhang, H. Zhan, Y. Liu, Y. Wang, Y. Zheng, *Nano Energy,* 2019, **60**, 127.
16. G. Yu, J. Hu, J. Tan, Y. Gao, Y. Lu, F. Xuan, F, *Nanotechnology,* 2019*,* **29**, 115502.
17. X. Lu, J. Yang, L. Qi, W. Bao, L. Zhao, R. Chen, *Sensors,* 2019*,* **19**, 794.
18. L. Zhao, F. Qiang, S.-W. Dai, S.-C. Shen, H. Shen, Y.-Z. Huang, N.-J. Huang, G.-D. Zhang, L.-Z. Guan, J.-F. Gao, Y. Song, L.-C. Tang, *Nanoscale,* 2019, **11**, 10229.
19. K. Kim, M. Jung, S. Jeon, J. Bae, *Smart Mater. Struct,*. 2019, **28**, 065019.
20. P. Li, L. Zhao, Z. Jiang, M. Yu, Z. Li, X. Zhou, Y. Zhao, *Sci. Rep.,* 2019, **9**, 14457.
21. X. Wang, Y. Gu, Z. Xiong, Z. Cui, T.; Zhang, *Adv. Mater.,* 2014, **26**, 1336.
22. S. Gong, W. Schwalb, Y. Wang, Y. Chen, Y. Tang, J. Si, B. Shirinzadeh, W. Cheng, *Nat. Commun.,* 2014, **5**, 3132.